

## Article

# A Comprehensive Evaluation of Different Power Quantities in DC Electric Arc Furnace Power Supplies

Pegah Hamedani <sup>1,\*</sup>, Cristian Garcia <sup>2</sup> and Jose Rodriguez <sup>3</sup>

<sup>1</sup> Department of Railway Engineering & Transportation Planning, University of Isfahan, Isfahan 8174673441, Iran

<sup>2</sup> Department of Electrical Engineering, Universidad de Talca, Curico 3340000, Chile

<sup>3</sup> Faculty of Engineering, Universidad San Sebastian, Santiago 4080871, Chile

\* Correspondence: p.hamedani@eng.ui.ac.ir

**Abstract:** Conventionally, DC arc furnaces are fed by thyristor rectifiers to control the level of current or power transferred to the load. With the advancement of high-power transistors, other structures such as diode rectifiers and DC choppers have been introduced and developed for the feeding system of DC electric arc furnaces. In this paper, the effect of different power supply systems on power quality indexes is discussed. In this regard, two types of feeding systems are considered, including a power supply system based on thyristor rectifiers and a power supply system based on diode rectifiers and DC choppers. In addition, different control methods, including constant current control (CCC) and constant power control (CPC), on DC electric arc furnaces are applied. For evaluating the power quality indexes, voltage and current harmonic distortion, unbalance of voltage and current, and power factor on the AC side are investigated for different power supply systems. Simulation results were performed with PSCAD/EMTDC software. It is shown that the power supply systems with diode rectifiers and DC choppers have superiority in comparison to the types based on thyristor rectifiers. According to the results, the average current THD is reduced from 16.55% in the thyristor rectifier to 8.40% in the chopper rectifiers with the CCC method and from 19.27% in the thyristor rectifier to 7.38% in the chopper rectifiers with the CPC method. Moreover, the average voltage THD is reduced from 5.67% in the thyristor rectifier to 3.02% in the chopper rectifiers with the CCC method. The result is similar to the CPC method. Furthermore, for a specific power supply system, the harmonic distortion is lower in the case of the CPC method than in the CCC method.

**Keywords:** DC electric arc furnace; feeding system; harmonic distortion; power quality; total harmonic distortion; unbalance



**Citation:** Hamedani, P.; Garcia, C.; Rodriguez, J. A Comprehensive Evaluation of Different Power Quantities in DC Electric Arc Furnace Power Supplies. *Energies* **2023**, *16*, 3888. <https://doi.org/10.3390/en16093888>

Academic Editor: J. C. Hernandez

Received: 26 March 2023

Revised: 18 April 2023

Accepted: 24 April 2023

Published: 4 May 2023



**Copyright:** © 2023 by the authors. Licensee MDPI, Basel, Switzerland. This article is an open access article distributed under the terms and conditions of the Creative Commons Attribution (CC BY) license (<https://creativecommons.org/licenses/by/4.0/>).

## 1. Introduction

With rapid advances in semiconductor technology and the improved performance of high-power AC/DC converters, DC electric arc furnaces have become increasingly popular among steel producers. In these furnaces, a DC current flows through the molten material and the arc, and the current circuit is closed through the graphite electrodes. The main characteristic of these loads is the rapid changes in the absorbed power, which happens especially in the first stage of melting. During this stage, the arc has critical conditions; because the arc is unstable, it continuously becomes a short circuit and an open circuit. These furnaces have all the functional advantages of AC electric arc furnaces, which have been obtained as a result of the evolution of electrical designs and metallurgical processes. In addition, DC arc furnaces are preferable to AC electric arc furnaces from different aspects such as the amount of electrode consumption, energy consumption, control of voltage flicker, movement and mixing of materials, melting in molten bath, fewer network disturbances, and better heat distribution [1].

Until now, various structures have been presented for the feeding system of DC electric arc furnaces, which can be classified into two main categories. The first category

includes power sources based on thyristor rectifiers, and the second category includes power sources based on diode rectifiers with DC–DC converters. According to the literature, some of the challenges that DC electric arc furnaces face include voltage and current harmonic distortion, voltage unbalance, load fluctuation, voltage flicker in the point of common coupling (PCC), and reactive power consumption [2,3]. So far, many articles have concentrated on solving the mentioned issues.

By using a suitable control method for the arc furnaces with a DC chopper feeding system, the adverse effects of flicker can be compensated, and the performance of the furnace can be improved. This solution is based on the constant power control method [4]. The most important advantage of this method is that it does not need any reactive power static compensator or static synchronous compensator for the operation of the furnace [5]. In furnaces with feeding systems based on thyristor rectifiers, many active devices including active filters, static synchronous compensators, and individual compensators have been studied to compensate the disturbances caused by furnace performance. In [5], the effectiveness of the above compensators in improving the waveform distortions and voltage fluctuations in the presence and absence of compensators is evaluated and compared.

Many articles have discussed the power quality issues of DC and AC electric arc furnaces [6–18]. However, most of the research has been in the field of AC electric arc furnaces [6–10]. In [12], IGBT-based rectifiers and thyristor-based rectifiers are compared for DC electric arc furnace plants in terms of dynamic response, arc stability, and THD index. Results manifest that IGBT-based rectifiers result in higher power quality than thyristor-based systems. However, thyristor-based rectifiers are usually more reliable and have lower costs. In [13], the definitions of power quality indexes in unbalanced and non-sinusoidal conditions are investigated. In [14], the effect of using multi-phase transformers in the supply system of DC electric arc furnaces is studied. In this research, power quality indexes such as harmonic distortion, unbalance, and voltage flicker are taken into account. Results show that increasing the phase numbers reduces the harmonic distortion and voltage unbalance. However, it does not affect the flicker intensity. In [15], the harmonic distortion at the power grid side is investigated in the presence of DC arc furnace loads. The experimental results of a 12-ton DC electric arc furnace are presented. Harmonic and interharmonic components of the line current are extracted at different stages of melting. In [16], the power quality indexes are studied at PCC between the DC electric arc furnace load and the power grid. In this work, power quality indexes including total harmonic distortion (THD), total interharmonic distortion (TIHD), or overall total harmonic distortion (OTHD) are calculated. Moreover, harmonic and interharmonic components have been taken into account in analyzing the frequency domain. In [17], the performance of different chaotic models including Chua, Lorenz, and Rössler is assessed based on the power quality indexes of the DC electric arc furnace loads. Power quality indexes including THD, TIHD, normalized instantaneous distortion energy (NIDE) ratio, and the short-term flicker severity ( $P_{st}$ ) are considered in this work. Due to the time-varying nature of the current and voltage waveforms and with the existence of interharmonics, in the DC electric arc furnace load, the NIDE is evaluated as an advanced power quality index based on time–frequency analysis of the signals, and using a wavelet transform, the calculation burden is decreased. In [19], new power definitions are presented to study the behavior of DC electric arc furnaces, including harmonics and unbalance. For this purpose, non-fundamental apparent power, non-active power, power factor, and unbalanced fundamental apparent power are determined to evaluate the load behavior.

According to the above-mentioned, the main aim of this work is to evaluate the power quality issues using the power definitions in different feeding systems of the DC electric arc furnace. In this work, the power supply systems based on thyristor rectifiers and diode rectifiers with DC–DC converters are presented. In addition, different control methods for the DC–DC converters, including duty cycle control by applying firing pulses at certain intervals, single-carrier pulse width modulation (SC-PWM) method, and the pulse width modulation method with the phase-shifted carriers (PSC), are investigated. Then,

considering the chaos model for DC electric arc furnaces, these methods are implemented on a system containing DC electric arc furnaces. For power quality evaluation, the constant current control (CCC) and the constant power control (CPC) methods are utilized for the DC electric arc furnace systems. Finally, the results are compared.

## 2. Feeding System of DC Electric Arc Furnaces

### 2.1. Power Supply System Based on Thyristor Rectifiers

Figure 1 shows the feeding system of a DC electric arc furnace based on thyristor rectifiers. This system includes a DC electric arc furnace, fed by two six-pulse thyristor rectifiers parallel to each other (to form a twelve-pulse rectifier). The rectifiers are also connected to the PCC by transformers with  $\Delta/\Delta$  and  $Y/\Delta$  connections [14]. The power supply of DC electric arc furnaces must first convert the electrical energy of the network into a form that can be used in the melting process. The DC furnace power source must be able to convert high AC voltages into controlled low DC voltages. In addition, the performance of the DC furnace power source should be such that it minimizes the disturbances to the AC system with the highest reliability while delivering energy to the metal melting process.

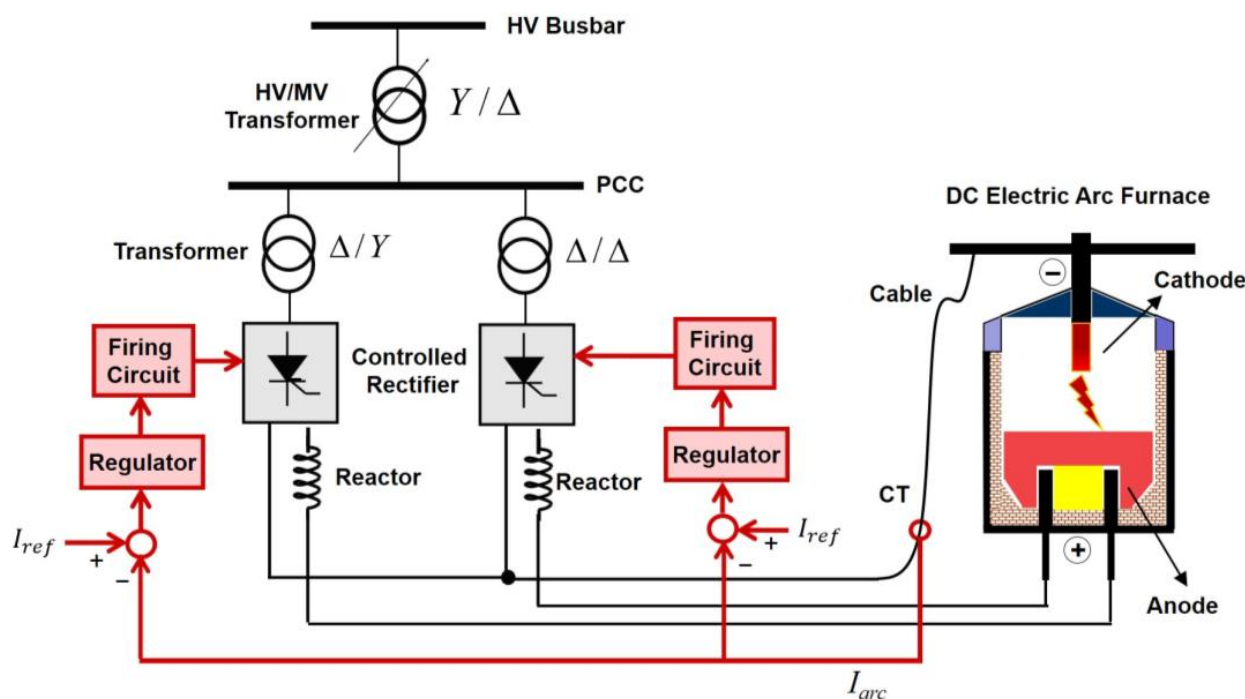


Figure 1. The feeding system of a DC electric arc furnace based on thyristor rectifiers.

To minimize the current harmonics on the AC side and to reduce the DC output ripple, usually, the power source of the furnace includes a twelve-pulse rectifier. Moreover, the outputs of the bridge circuits are connected in parallel to double the load-feeding current. An essential issue in the performance of twelve-pulse rectifiers is the absorption of reactive power due to the operation with a variable firing angle ( $\alpha$ ).

DC furnaces are usually fed by thyristor rectifiers to control the level of current or power delivered to the load. These furnaces are generally operated with CCC or CPC methods. The CCC method is typically used during the cold start-up of the furnace when the necessary conditions for the arc do not exist, and many jumps appear in the arc current. On the other hand, the CPC method is often used during the normal operation of the furnace [2].

The melting process is a continuous process and relies on constant power. To maintain a constant set point for arc current or power, proportional–integral (PI) controllers are used. The converter control system, with the help of PI controllers and the feedback loop,

produces appropriate firing pulses for the thyristors. It keeps the control variable of current or arc power at the desired value.

An optimal control system should guarantee the proper operation of the arc furnace and the quick response to electric arc fluctuations. Moreover, it should reduce the disturbances of the power injected into the grid. Due to the time-varying nature of the furnace load, fine-tuning the PI controller requires extensive studies of non-linear, time-varying, and non-periodic systems. Since such studies involve a lot of difficulties, in practice, it is enough to adjust the approximate controller using the repetition method [19]. Figure 2 shows the block diagram of the control scheme for the power supply system based on thyristor rectifiers, for the CCC method.

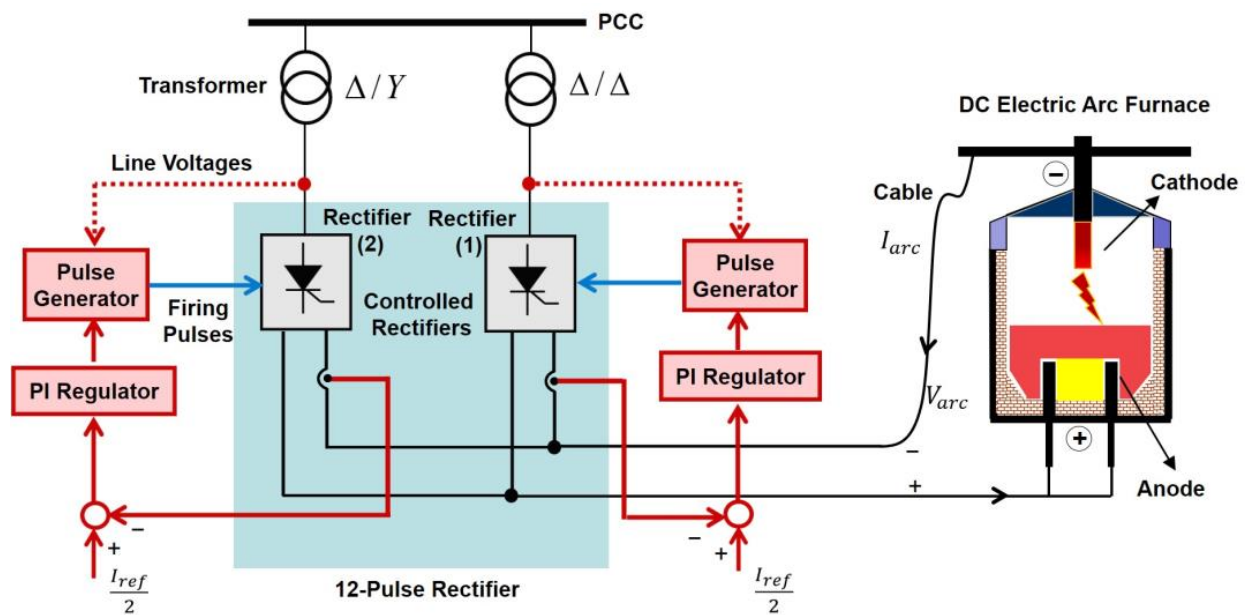


**Figure 2.** Block diagram of the control scheme for the power supply system based on thyristor rectifiers with the CCC method.

Figure 3 shows a block diagram of the control scheme with CCC and CPC methods. The CCC method is represented in Figure 3a for a rectifier. DC electric arc furnaces are usually utilized with constant current or power control methods. The constant current control method is usually used during cold start-ups in which there is a lack of arc condition and multiple arc current peaks. Likewise, the constant power control method is most often used during normal operation since smelting is a continuous process that relies on constant power. To maintain a constant set point, feedback PI controllers are usually used. Because of the fluctuation of the current at the beginning of the smelting (boring stage), the constant current control strategy is used at this stage. The output current of each rectifier is measured and passed through a first-order low-pass filter with a gain of 1 and a time constant of 0.3 msec.

Then, after comparing with a set-point current, a PI regulator with a limiter is utilized to produce the firing angle of the rectifier. The CPC method is shown in Figure 3b for a rectifier. The output current and voltage of each rectifier are measured and passed through a low-pass filter with a gain of 1. Then, after multiplying these two signals, it is compared with a set-point power. By applying a PI regulator with a limiter, the firing angle of the rectifier is produced.

The most important advantages of the thyristor power supply system are high efficiency, high reliability, proper load current control, and low cost. Its disadvantages include high input reactive power, generation of current harmonics, voltage notch, use of power filters, and output current ripple [20].

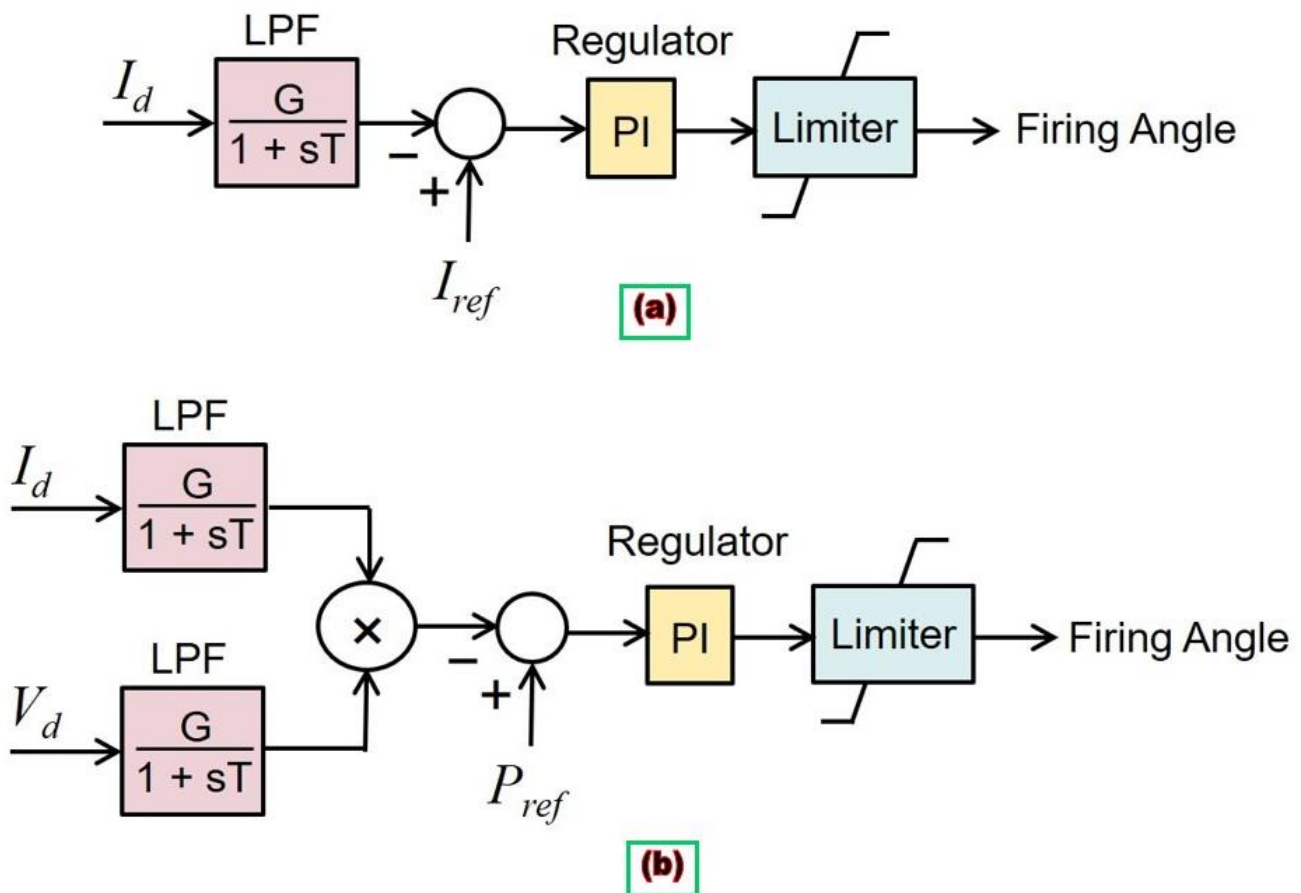


**Figure 3.** Block diagram of the control scheme for the power supply system based on thyristor rectifiers with: (a) CCC method; (b) CPC method.

## 2.2. Power Supply System Based on Diode Rectifiers with DC Choppers

With the advancement of high-power transistors, another structure for a DC electric arc furnace feeding system, including the combination of diode rectifiers and DC choppers, was considered. Figure 4 shows the block diagram of a DC electric arc furnace with a feeding system based on diode rectifiers and DC choppers. This type of power source includes transformers related to rectifiers, diode bridge rectifiers, DC choppers, and output reactors. In this feeding system, with the use of diode rectifiers, the low AC voltage in the secondary of the transformers is converted to a constant low DC voltage at the output of the rectifier. Then, the choppers convert this constant DC voltage to a controlled low DC voltage at the output of the converter [14].

The power source based on DC choppers uses IGBT semiconductor switches as the controlled element. The used DC chopper is a buck regulator type, and the current can only pass in one direction. The circuit structure of the utilized DC–DC converter includes an input capacitor, a transistor switching element, and a freewheeling diode. In high-current applications, a sufficient number of these units must be paralleled to provide the required current. Input DC link capacitors provide a constant DC voltage at the input of chopper units. Since it is assumed that the load has an inductive characteristic, the freewheeling diode must provide a path for the energy released by the load inductance when the semiconductor switch is turned off. As an added protection, a fast-acting anti-parallel diode is connected with the IGBT to direct the current in the opposite direction. A detailed structure of the power supply system based on diode rectifiers and buck choppers is presented in Figure A1 in Appendix A.

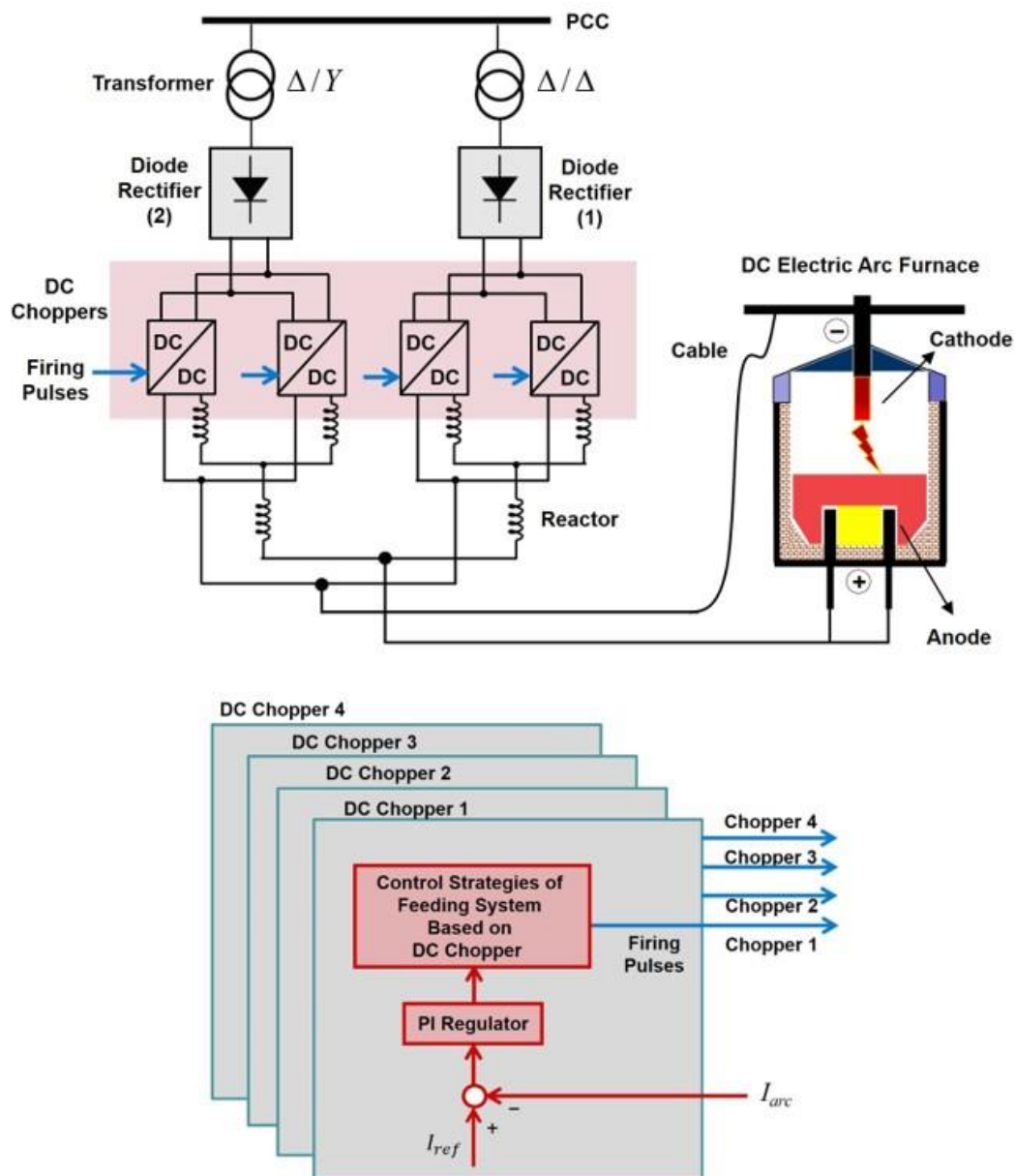


**Figure 4.** The structure of a DC arc furnace with a feeding system based on diode rectifiers and DC choppers.

### 3. Control Strategies of Feeding System Based on DC Chopper

#### 3.1. Duty Cycle Control Method with Firing Pulses at Certain Intervals

In this method, the switching period ( $T_s$ ) of the IGBT is divided into  $n$  equal intervals according to the number of available chopper units ( $n$ ). In this research, four chopper units were considered. Therefore,  $T_s$  is divided into four equal parts. In general, the number and type of elements that conduct in each time interval  $T_s/n$  depend on the duty cycle ( $D$ ). It can be said that each time interval  $T_s/n$  can be divided into two sub-intervals. These two sub-intervals are  $T_x$  and  $T_y$ , which, respectively, represent the duration in which the  $m$ -th and  $(m - 1)$ -th IGBT switches conduct. Time intervals  $T_x$  and  $T_y$  can be obtained by using Equations (1) and (2), respectively.

$$T_x = \left( D - \frac{m-1}{n} \right) T_s \tag{1}$$

$$T_y = \frac{T_s}{n} - T_x \quad (2)$$

In the above equations,  $n$  is the number of chopper units, and  $m$  can be obtained from the following inequality:

$$\frac{m-1}{n} < D \leq \frac{m}{n} \quad (3)$$

### 3.2. Single-Carrier Pulse Width Modulation (SC-PWM)

In the SC-PWM method, firing signals are generated by comparing a control signal ( $V_{Control}$ ), called a reference signal, with a triangular carrier waveform ( $V_{tri}$ ) with a frequency of  $f_s$ . The carrier frequency  $f_s$  is the same as the IGBT switching frequency. As shown in Figure 5, when the control signal is greater than the triangular carrier signal, the output of the comparator will be equal to one. Otherwise, the output will be equal to zero. In this way, by changing the reference signal, the duty cycle can be controlled to achieve specific goals in the operation of DC electric arc furnaces, either by controlling the constant current or the constant power of DC electric arc furnaces. In the SC-PWM method, to create firing signals, a triangular carrier signal is used for all four units, and a distinct reference signal is considered for each unit.

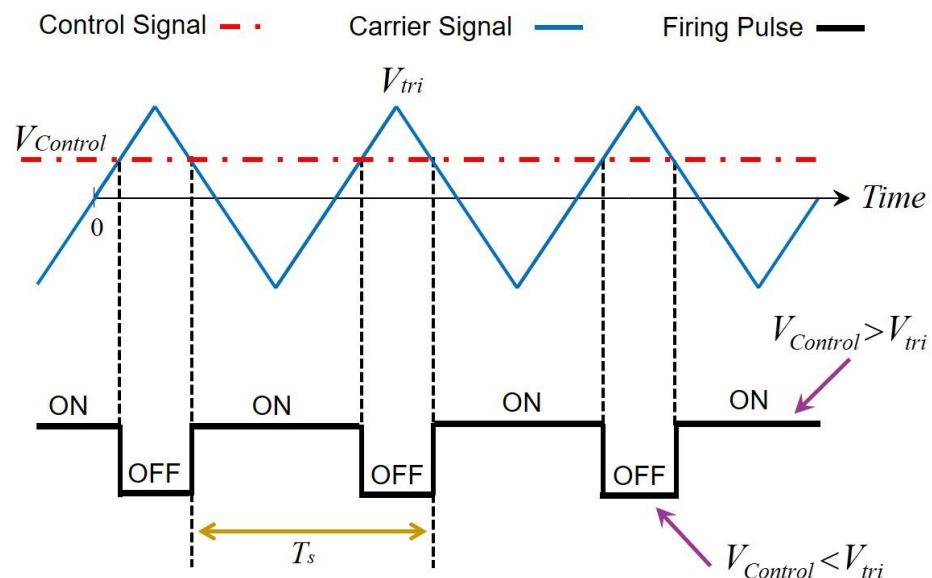


Figure 5. PWM strategy.

In the arc furnace control process with a constant current or constant power approach, the reference signal and the duty cycle of the circuit units are controlled to reach the constant arc current or power. The disadvantage of this method is that if the control of the chopper units with the same work cycles is considered, all the chopper units will be turned off during periods, and no power will be transferred from the source to the furnace; rather, in this case, the energy of the arc is provided by the energy stored in the output inductors of the chopper converters. As a result, to prevent sudden drops or discontinuity of the current, the inductance value of the output inductors must be large enough, which will lead to an increase in the cost of the power supply system.

### 3.3. Pulse Width Modulation Method with Phase-Shifted Carriers (PSC)

This method is similar to the SC-PWM method, with the difference that instead of using a triangular carrier signal, we will have triangular carrier signals that have a phase shift relative to each other in the number of units. Therefore, in this research, the number of carrier signals will be four. Each of these carrier signals is specific to one of the available

chopper units. Figure 6 shows the triangular carrier signals with proper phase transition and the corresponding chopper units.

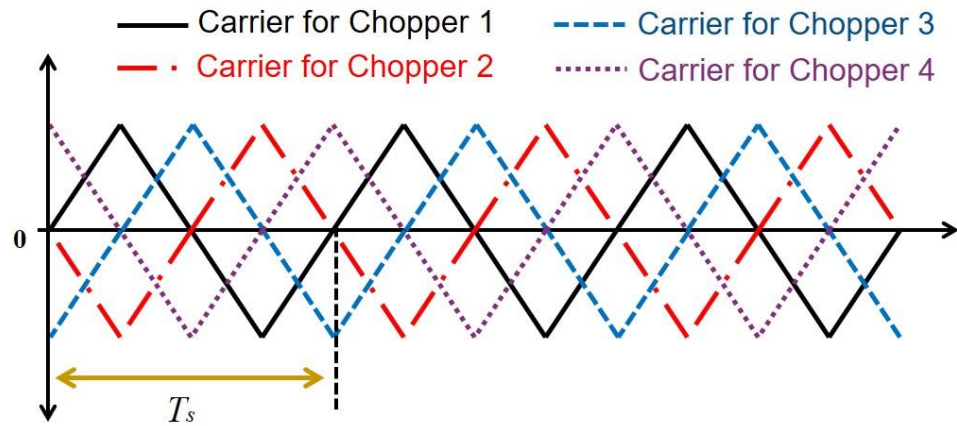


Figure 6. Triangular phase-shifted carrier signals and the corresponding chopper units.

In this method, a distinct reference signal is considered for each of the chopper units. In the arc furnace control process with the CPC approach, the reference signal and, accordingly, the duty cycle of the chopper units are controlled to reach constant current or constant power.

The advantage of this method compared to the SC-PWM approach is that if the chopper units are controlled with the same duty cycles, for  $D > 0.25$ , the turn-off problem of all the chopper units and consequently not transferring power to the furnace in specific periods does not occur. This fact is shown in Figure 7a. As can be deduced from Figure 7b, the above problem will still exist for  $D < 0.25$ ; however, due to the minimization of losses according to the circuit topology, the power source is usually used with a duty cycle in the range of  $0.6 < D < 0.8$ , in which this issue will not be significant. Another advantage of this method compared to the SC-PWM method is that, in this method, the multiple numbers of carriers that have a phase shift with respect to each other helps to spread the start times of the control units during the switching period ( $T_s$ ). This, in turn, will cause the uniform transfer of power to the arc furnace, and on the other hand, it will prevent the occurrence of severe voltage fluctuations on the primary side of the rectifier transformers.

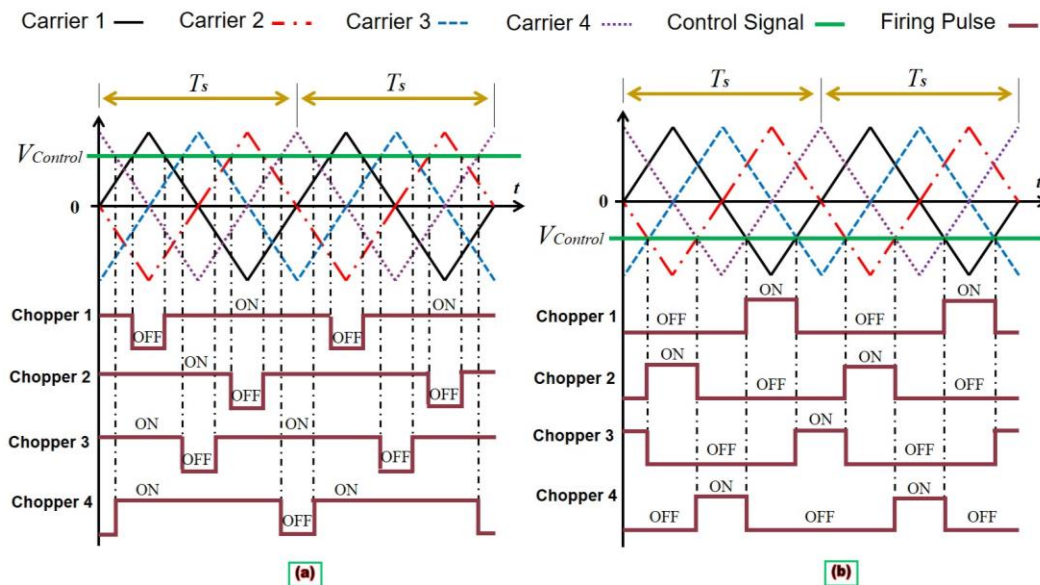


Figure 7. Control of chopper units with equal duty cycles for: (a)  $D > 0.25$ ; (b)  $D = 0.25$ .

#### 4. Power Quality Indexes in Unbalanced and Non-Sinusoidal Conditions

In this section, the definitions related to unbalanced and non-sinusoidal environments are reviewed [21]. In a single-phase system in non-sinusoidal conditions, the instantaneous voltage and current can be expressed according to the following equations:

$$v(t) = V_0 + \sqrt{2} \sum_{h \neq 0}^{\infty} V_h \cos(h\omega t + \phi_h) \quad (4)$$

$$i(t) = I_0 + \sqrt{2} \sum_{h \neq 0}^{\infty} I_h \cos(h\omega t + \varphi_h) \quad (5)$$

In the above equations,  $\omega$  is the angular frequency of the fundamental component,  $V_0$  and  $I_0$  are the dc components, and  $V_h$  and  $I_h$  are the amplitudes of the  $h$ -th order harmonics of the voltage and current, respectively. The root-mean-square (RMS) values of the above voltage and current waveforms can be obtained using the following equations:

$$V_{RMS} = \sqrt{\sum_{h=0}^{\infty} V_h^2} \quad (6)$$

$$I_{RMS} = \sqrt{\sum_{h=0}^{\infty} I_h^2} \quad (7)$$

The active and reactive power of each harmonic can be obtained as follows:

$$P_h = V_h I_h \cos \theta_h \quad (8)$$

$$Q_h = V_h I_h \sin \theta_h \quad (9)$$

where  $\theta_h$  is the phase difference between the voltage and current harmonics of the  $h$ -th order.

In a three-phase four-wire system, the RMS values of voltage and current can be expressed according to the following equations:

$$V = \left[ \frac{(V_a^2 + V_b^2 + V_c^2)}{3} \right]^{\frac{1}{2}} \quad (10)$$

$$I = \left[ \frac{(I_a^2 + I_b^2 + I_c^2)}{3} \right]^{\frac{1}{2}} \quad (11)$$

where  $I_a$ ,  $I_b$ , and  $I_c$  are the RMS values of three-phase currents considering the harmonic components.  $V_a$ ,  $V_b$ , and  $V_c$  are the RMS values of three-phase voltages considering the harmonic components.

By using the RMS values obtained from Equations (10) and (11), the equivalent apparent power can be obtained as:

$$S = 3VI \quad (12)$$

The fundamental component of voltage and current can be computed as follows:

$$V_1 = \left[ \frac{(V_{a1}^2 + V_{b1}^2 + V_{c1}^2)}{3} \right]^{\frac{1}{2}} \quad (13)$$

$$I_1 = \left[ \frac{(I_{a1}^2 + I_{b1}^2 + I_{c1}^2)}{3} \right]^{\frac{1}{2}} \quad (14)$$

Equivalent harmonic components for voltage and current can also be calculated from the following equations:

$$V_H = \left[ \frac{(V_{ah}^2 + V_{bh}^2 + V_{ch}^2)}{3} \right]^{\frac{1}{2}} \quad (15)$$

$$I_H = \left[ \frac{(I_{ah}^2 + I_{bh}^2 + I_{ch}^2)}{3} \right]^{\frac{1}{2}} \quad (16)$$

With the help of the fundamental component of voltage and current, the fundamental apparent power can be obtained as:

$$S_1 = 3V_1I_1 \quad (17)$$

The non-fundamental apparent power can be expressed as follows:

$$S_N = \sqrt{S^2 - S_1^2} \quad (18)$$

The non-fundamental apparent power indicates the amount of load power distortion. Another expression that can be expressed in non-sinusoidal conditions is as follows:

$$S^2 = P^2 + Q^2 + D^2 \quad (19)$$

where  $D$  is the distortion power.  $P$  and  $Q$  can be written as:

$$P = P_1 + P_H, \quad Q = Q_1 + Q_H \quad (20)$$

in which the fundamental and harmonic components are as follows:

$$\begin{aligned} P_1 &= P_{a1} + P_{b1} + P_{c1} \\ P_H &= \sum_{h \neq 1} (P_{ah} + P_{bh} + P_{ch}) \\ Q_1 &= Q_{a1} + Q_{b1} + Q_{c1} \\ Q_H &= \sum_{h \neq 1} (Q_{ah} + Q_{bh} + Q_{ch}) \end{aligned} \quad (21)$$

The non-active power  $N$  is also defined as follows:

$$N = \sqrt{S^2 - P^2} \quad (22)$$

In an unbalanced system, the active and reactive power of the fundamental positive sequence can be defined as:

$$P_1^+ = 3V_1^+ I_1^+ \cos\theta_1^+ \quad (23)$$

$$Q_1^+ = 3V_1^+ I_1^+ \sin\theta_1^+ \quad (24)$$

where  $V_1^+$  and  $I_1^+$  are the fundamental components of the positive sequence. The apparent power of the fundamental positive sequence is defined as follows:

$$S_1^+ = 3V_1^+ I_1^+ \quad (25)$$

In addition, the fundamental apparent power in the unbalanced condition can be defined as follows:

$$S_{u1} = \sqrt{S_1^2 - S_1^{+2}} \quad (26)$$

Finally, the total power factor is defined as follows:

$$PF = \frac{P}{S} \quad (27)$$

The displacement power factor, in which only the fundamental components are considered, is defined as:

$$dPF = \frac{P_1}{S_1} \quad (28)$$

The displacement power factor of the positive sequence is written as follows:

$$dPF^+ = \frac{P_1^+}{S_1^+} \quad (29)$$

## 5. Simulation Results and Discussion

### 5.1. Simulation of the Feeding System for the DC Electric Arc Furnace

To investigate the effect of different control methods of power supply systems based on diode rectifiers with DC–DC converters, the system shown in Figure 4 is simulated using PSCAD/EMTDC software. The simulation parameters are taken from [2]. It should be mentioned that in this simulation, the DC electric arc furnace chaos model was used. The Lorenz chaotic model of DC electric arc furnaces is presented in Appendix B [22]. The simulation time step is considered equal to 20  $\mu$ s.

Furthermore, different control strategies of the feeding system based on DC chopper were discussed in Section 3, and the following were applied:

- Method 1: duty cycle control method with firing pulses at certain intervals.
- Method 2: SC-PWM.
- Method 3: PWM Method with PSC.

Figure 8 shows the total input current on the AC side in the above three control methods. These currents have been obtained for a constant duty cycle of  $D = 0.8$ . It is clear that in PWM methods, in conditions where the maximum value of the carrier wave is equal to one, a duty cycle of  $D = 0.8$  is provided for  $V_{Control} = 0.6$ . As can be seen, these methods have relatively similar behavior from the point of view of the AC network. The similarity in the absorbed currents from the network in these three methods acknowledges that the power quality effects in the network are almost similar to each other.

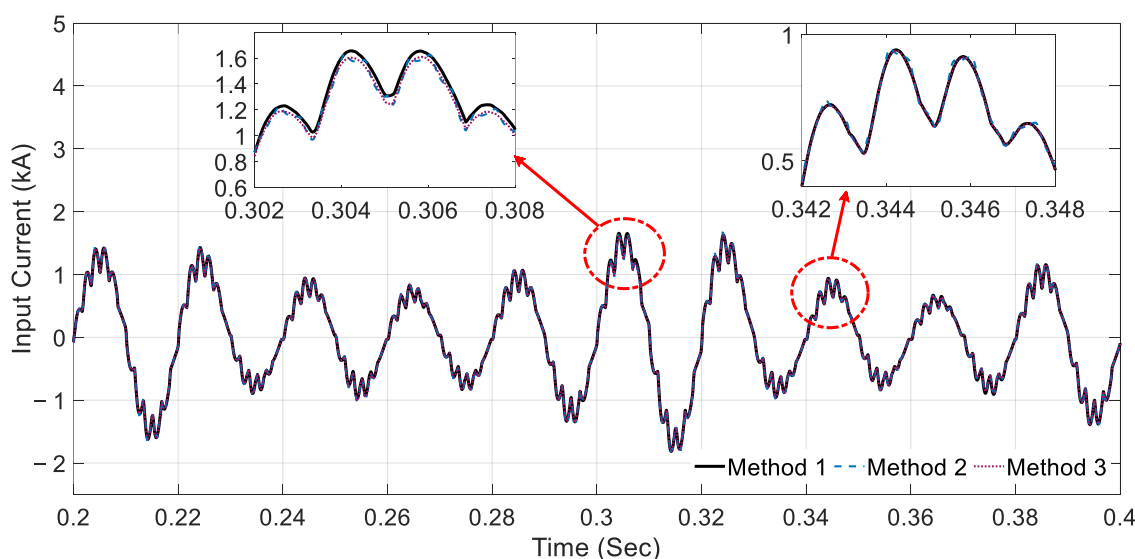


Figure 8. The input current on the AC side of the feeding system with different control methods.

Figure 9 shows the input current of one of the rectifiers in the three mentioned methods with the duty cycle of  $D = 0.8$ . As can be seen, the results of these three methods have slight deviations from each other.

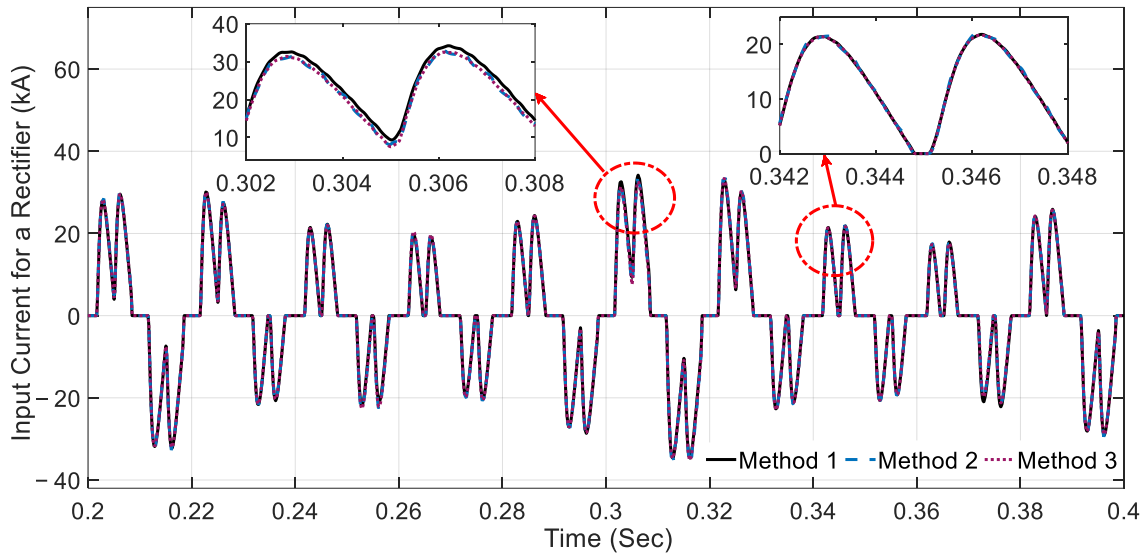


Figure 9. The input current of a rectifier in the feeding system.

The input currents of chopper units 1 and 2 are shown in Figure 10a for the three discussed methods. In this case, the duty cycle of choppers is the same and equal to 0.8. As can be seen in this figure, the current waveforms of the chopper units in the first and third methods have many fluctuations. Figure 10b shows the input currents of chopper units 1 and 2 using a DC electric arc furnace with the CCC method in the three mentioned methods.

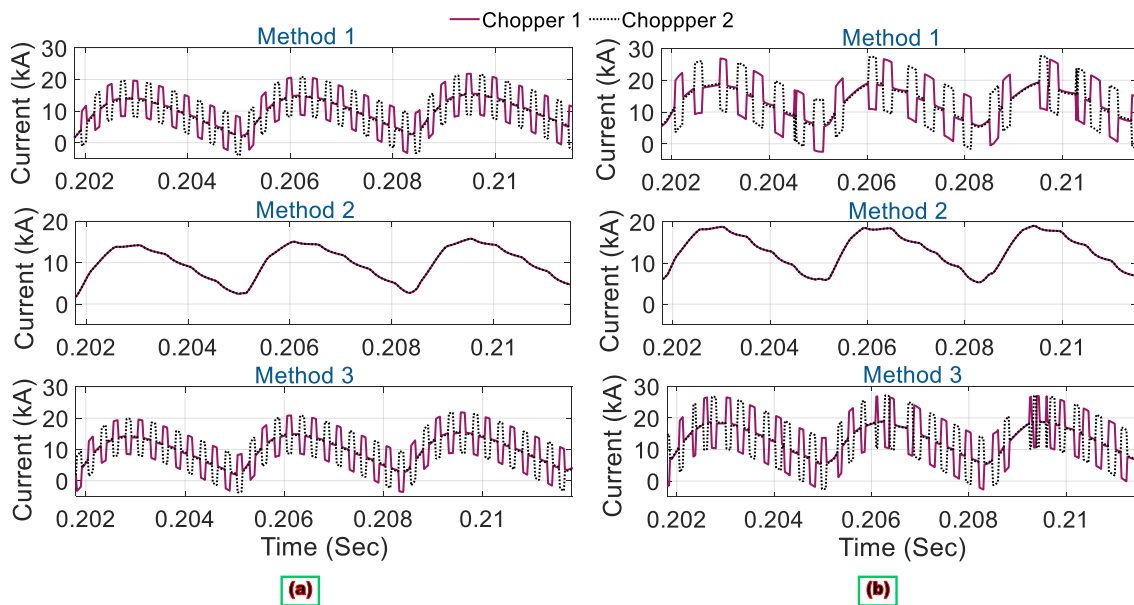
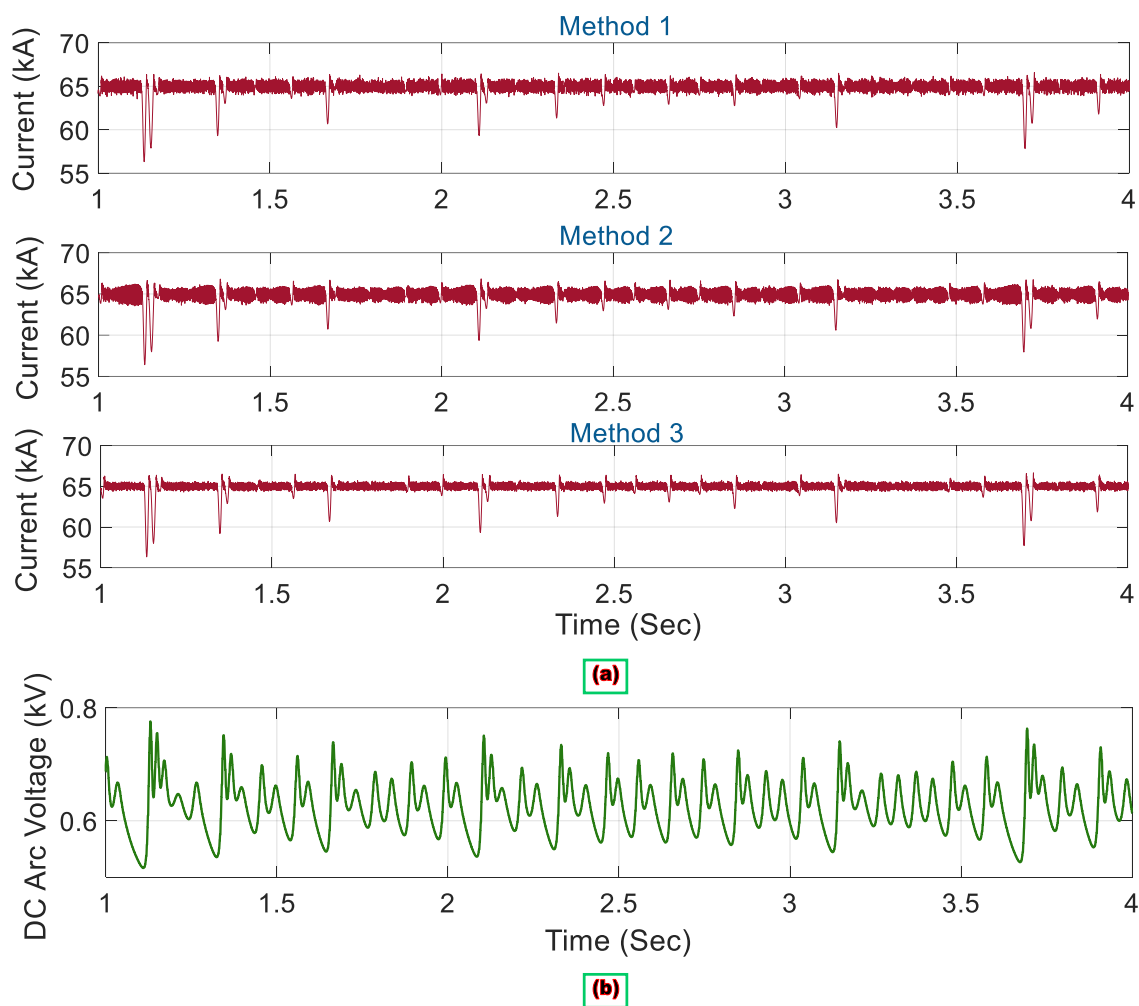


Figure 10. The input currents of choppers 1 and 2 with different control methods: (a)  $D=0.8$ ; (b) CCC method.

Moreover, Figure 11a represents the DC arc current for controlling the constant current of the arc furnace in the above three methods. The reference value of the arc current is considered equal to 65 kA, and the CCC method is applied to the studied DC electric arc

furnace. According to the simulation results, the third method will result in less deviation compared to the determined reference value.



**Figure 11.** (a) DC electric arc current to control the constant current of the arc furnace in the three discussed methods; (b) DC arc voltage.

During the operation of the electric arc furnace, severe voltage fluctuations cause current drops, short circuits, and sometimes an arc interruption [4]. In this regard, the severe and sudden drops in the arc current seen in Figure 11a refer to severe fluctuations in the arc voltage. Figure 11b shows the DC arc voltage in two different periods. It should be mentioned that this voltage is obtained from the chaos model of DC electric arc furnaces. As a result, it is clear that the PWM method with phase-shifted carriers has a smaller fluctuation range around the reference value. In addition, this method has advantages such as uniform power transfer to the furnace and preventing severe and sudden current drops in the primary side of rectifier transformers. Therefore, the PWM method with phase-shifted carriers is preferable in comparison to other methods.

### 5.2. Power Quality Evaluation of the DC Electric Arc Furnace Feeding Systems

In this part, the effect of the introduced conventional feeding systems, shown in Figures 1 and 4, on various power quality indexes are investigated. The utilized parameters are similar to Section 5.1. Due to the advantages of the PWM control method with given phase-shifted carriers, this control method has been used in the feeding system based on DC choppers.

Figure 12 shows the DC arc current of the feeding system based on the diode rectifiers with DC choppers and the thyristor rectifiers. The current reference is considered equal to 65 kA, and the CCC control is applied to the studied DC electric arc furnace. The results show that the chopper feeding system will result in a lower deviation compared to the reference value.

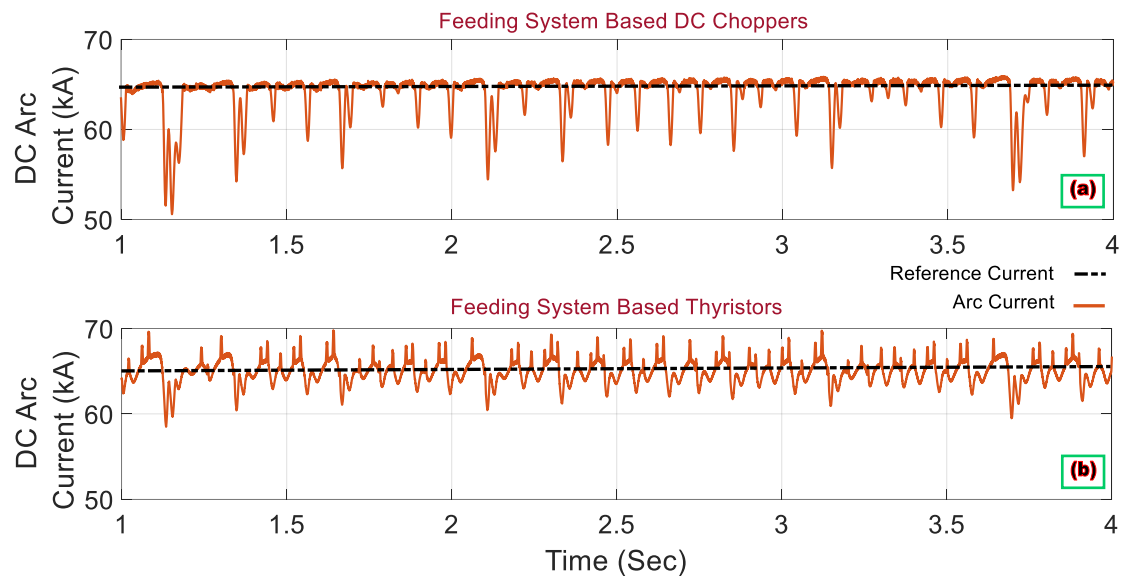


Figure 12. DC arc current in CCC control: (a) chopper rectifiers; (b) thyristor rectifiers.

Similarly, Figure 13 shows the arc power when applying the CPC method on the electric arc furnace feeding system based on the diode rectifiers with DC choppers and the thyristor rectifiers. For this purpose, Equation (20) was utilized. The power reference is considered equal to 40 MW. As can be seen in this figure, the convergence to the reference value is much more favorable in the chopper feeding system than in the thyristor feeding system.

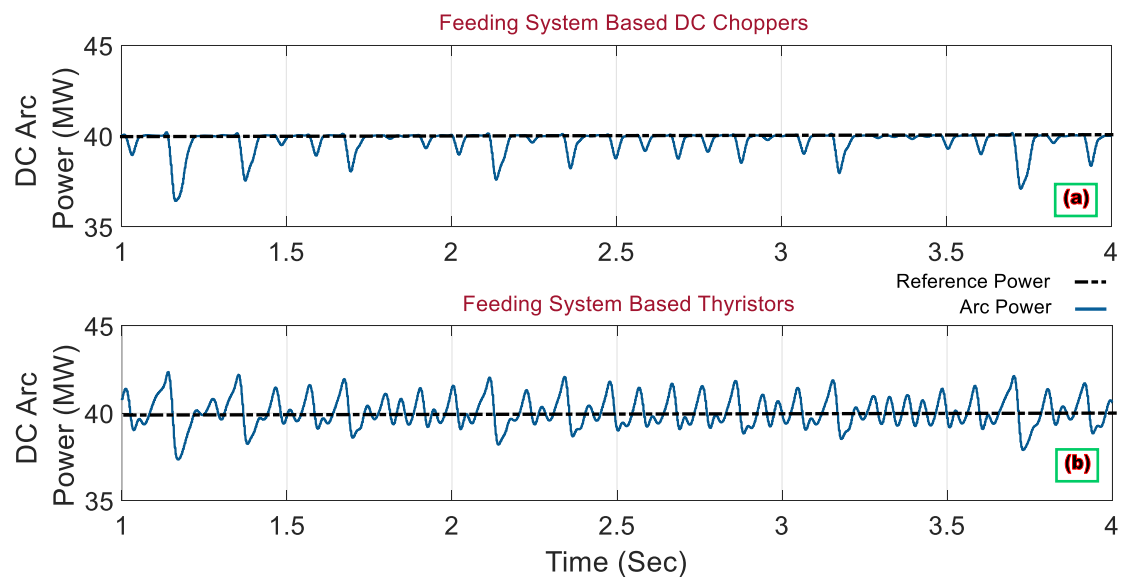
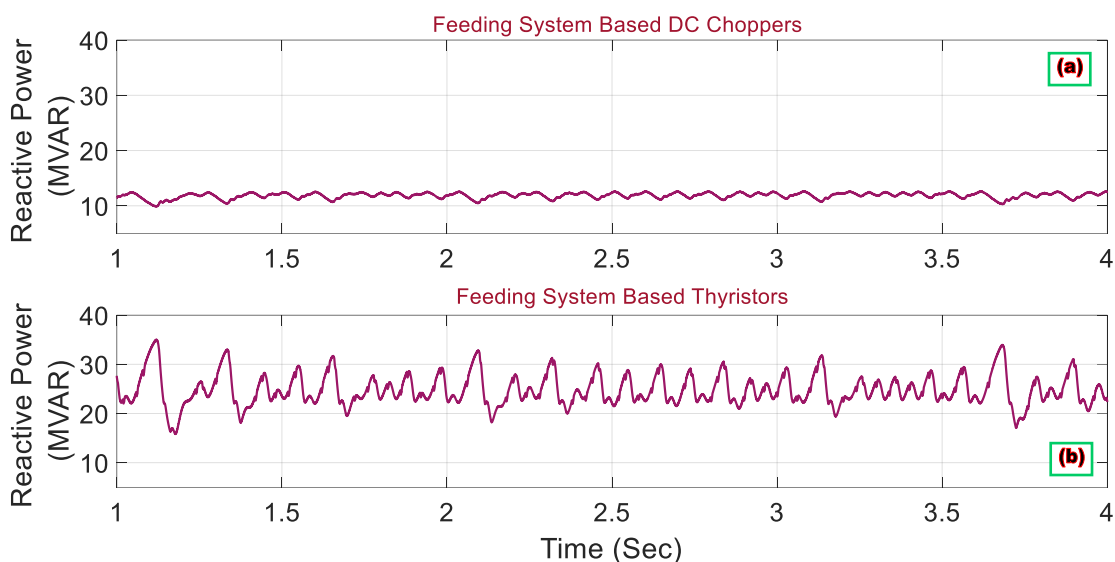


Figure 13. DC arc power in CCC control: (a) chopper rectifiers; (b) thyristor rectifiers.

Figure 14 illustrates the reactive power absorbed from the network using these two different feeding systems based on chopper units and thyristor power supply systems. For this purpose, Equation (20) was utilized. As can be seen, the reactive power consumption

has been significantly reduced in the feeding system based on the diode rectifiers with DC choppers. In addition, the reactive power fluctuations in the DC choppers power supply system are much less than the fluctuations of reactive power in the case of the thyristor power supply system. In fact, due to the high switching frequency of the chopper units, tracking the arc voltage fluctuations is performed faster. As a result, the active and reactive powers in this system have more uniformity and fewer fluctuations.



**Figure 14.** Reactive power of the grid connected to the DC arc system with CCC control: (a) chopper rectifiers; (b) thyristor rectifiers.

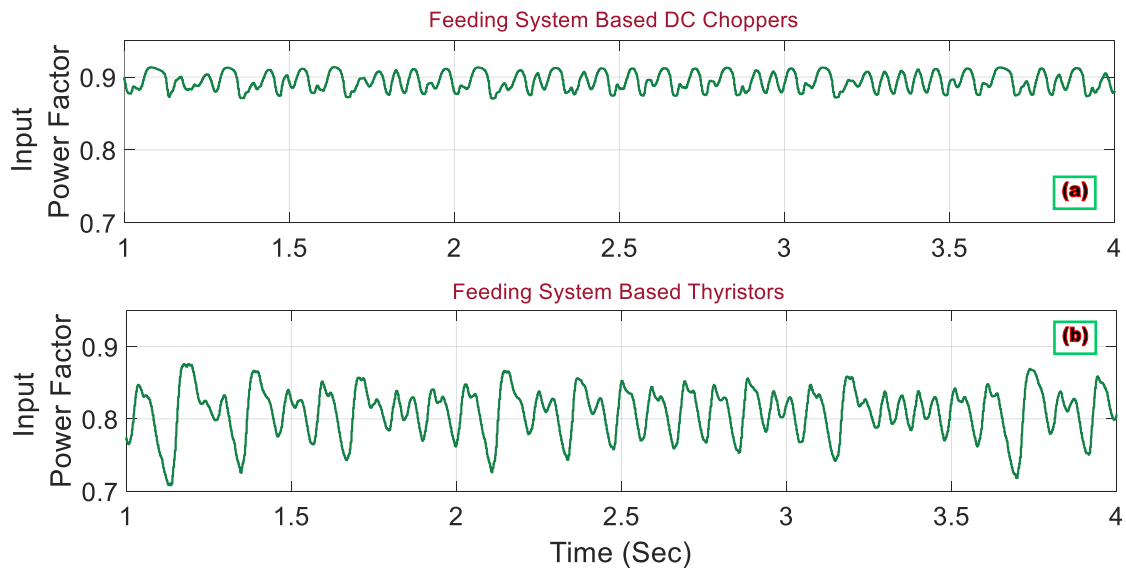
On the other hand, multiple chopper units ensure a balanced power distribution between diode rectifiers, and current control loops are also used for equal current distribution between chopper units. In addition, the balance of the current between the secondary of the transformers causes the elimination and weakening of the low-order harmonics. Therefore, the amount of absorbed reactive power and its fluctuations are reduced in this type of power supply system. As a result, there is no need for harmonic filters and reactive power compensation devices on the chopper side. Since reactive power fluctuations have a direct relationship with voltage fluctuations and consequently with the flicker intensity, it can be said that the flicker intensity is less in the case of a chopper power supply. Due to the significant reduction in the absorbed reactive power in the chopper power supply system, it is expected that the input power factor has also improved in this case. This is shown in Figure 15 for the CCC method applied to the studied electric arc furnace. For this purpose, Equation (27) was utilized.

The THD of the input current is shown in Figure 16 for the CCC method applied to the studied DC arc furnace system. It is clear that the THD was significantly reduced when using the power supply system based on chopper units.

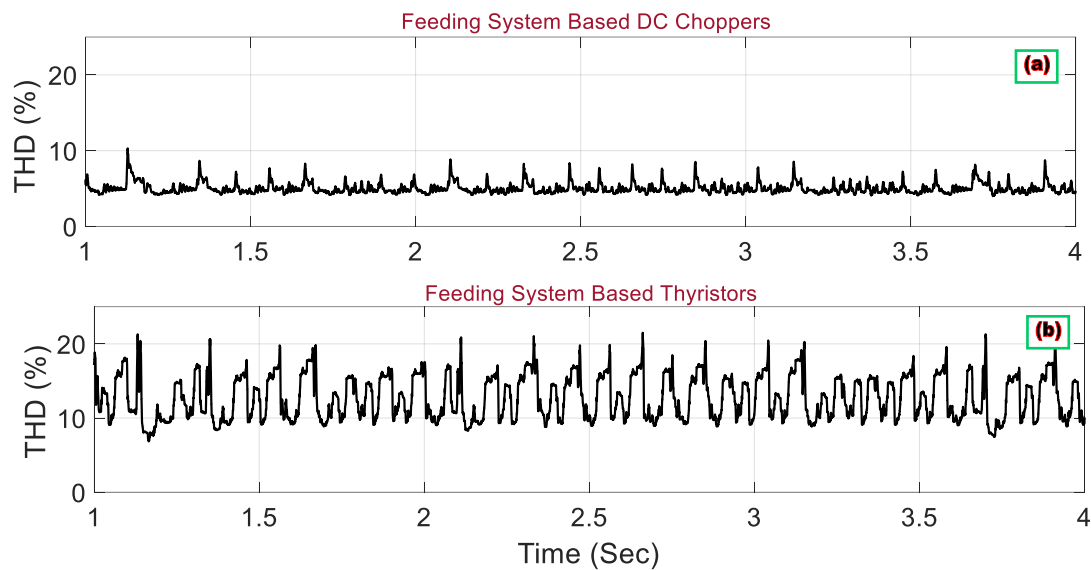
In Figures 17 and 18, the non-active power ( $N$ ) and the distortion power ( $D$ ) are shown for the two different feeding systems based on chopper units and thyristor power supply systems. For this purpose, Equations (22) and (19) were utilized, respectively. The CCC method was applied to both feeding systems. As can be seen, in the case of the chopper power supply system, the non-active and distortion powers have smaller values than the thyristor power supply system.

The non-fundamental apparent power  $S_N$  is related to the amount of harmonic distortion, and the  $S_N/S$  ratio is a suitable index to compare the amount of harmonic distortion created in different states of the power supply system [21]. Figure 19 shows the  $S_N/S$  index for the CCC method applied to the two different feeding systems based on chopper units and thyristor power supply systems. For this purpose, Equations (18) and (19) were used. As can be seen, the average value of this index in the case of the chopper feeding system is

lower than its average value in the case of the thyristor feeding system. This indicates that the harmonic distortion is less in the case of the chopper feeding system and is consistent with the result obtained from Figure 16.



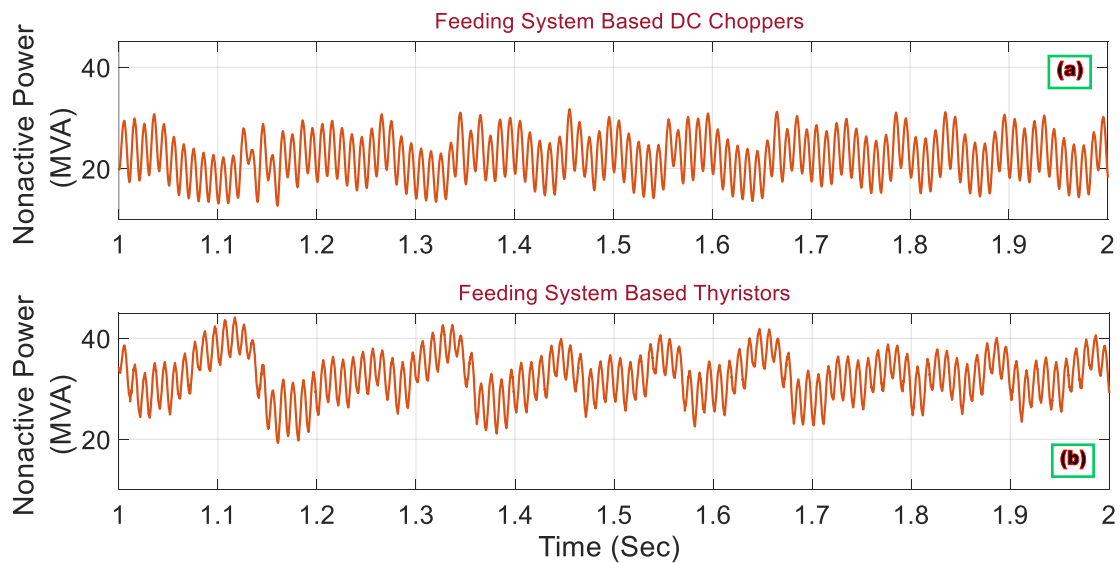
**Figure 15.** Input power factor of DC arc system with CCC control: (a) chopper rectifiers; (b) thyristor rectifiers.



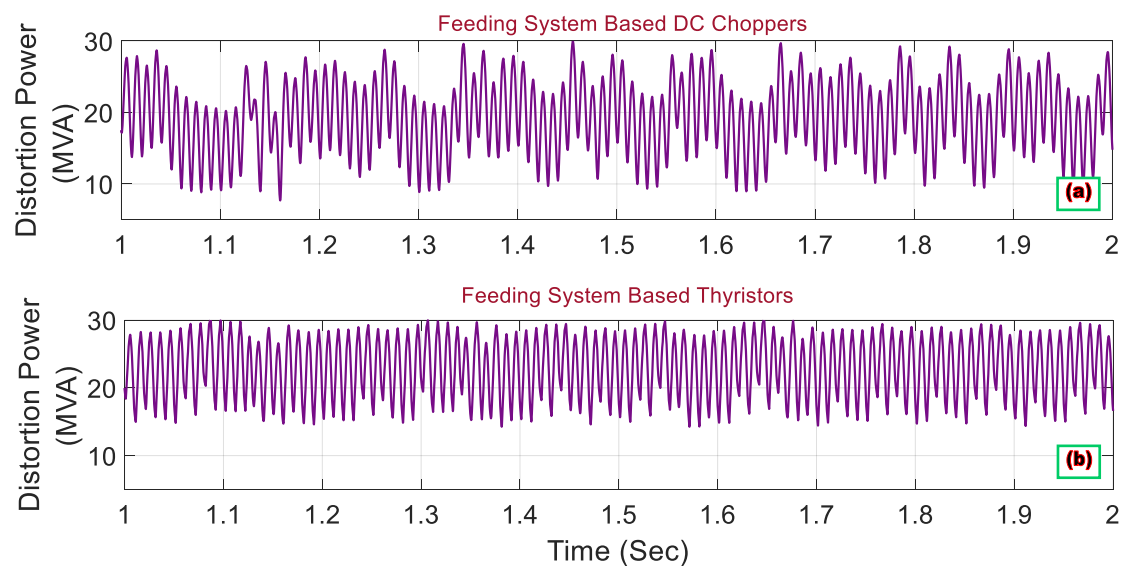
**Figure 16.** Input current THD of DC arc system with CCC control: (a) chopper rectifiers; (b) thyristor rectifiers.

Figure 20 compares the reactive power absorbed from the network in the two control methods of CCC and CPC for the power supply system based on chopper rectifiers. As can be seen, in the case of the feeding system with the CPC method, the reactive power fluctuations are less.

Figure 21 shows a comparison of the input power factor in the two control methods of CCC and CPC for the power supply system based on chopper rectifiers. As can be seen, in the CPC method that is often used during the normal operation of DC electric arc furnaces, power factor fluctuations are less.



**Figure 17.** Non-active power of DC arc system with CCC control: (a) chopper rectifiers; (b) thyristor rectifiers.



**Figure 18.** Distortion power of DC arc system with CCC control: (a) chopper rectifiers; (b) thyristor rectifiers.

Figure 22 illustrates a comparison of the input current THD in the two control methods of CCC and CPC for the power supply system based on chopper rectifiers. It is clear that in the CPC method, the current THD is lower than in the CCC method.

In Figures 23 and 24, non-active power ( $N$ ) and the distortion power ( $D$ ) are shown in the two control methods of CCC and CPC for the power supply system based on chopper rectifiers. As can be seen, in the case of the chopper power supply system, the non-active and distortion powers are slightly different for the CCC and CPC methods. In the CPC method, the maximum values of non-active and distortion power are less.

Figure 25 presents the  $S_N/S$  index in the two control methods of CCC and CPC for the power supply system based on chopper rectifiers. As can be seen, the average value of this index in the CPC method is lower than its average value in the CCC method. Moreover, in the CPC method, the maximum values of the  $S_N/S$  index are lower. This indicates that the harmonic distortion is less in the CPC method and is consistent with the result obtained from Figure 22.

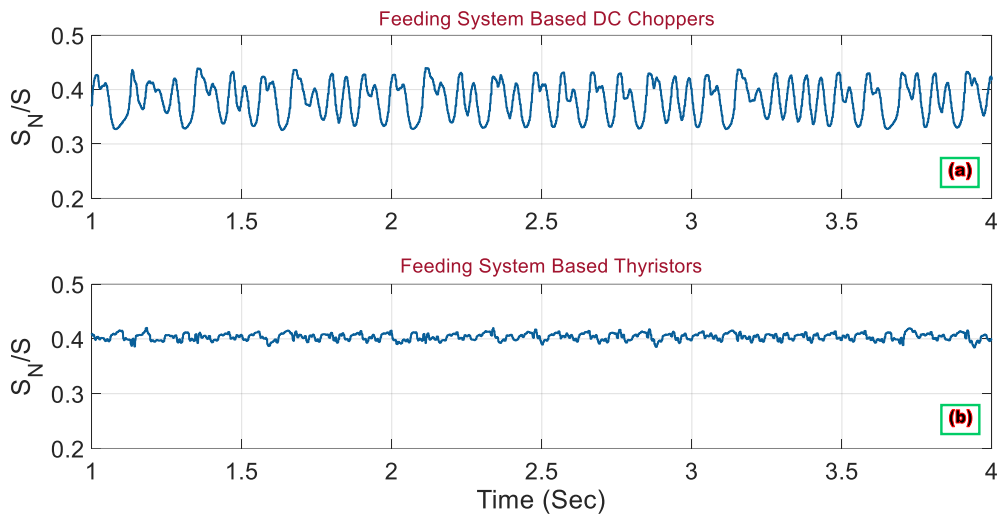


Figure 19.  $S_N/S$  index in DC arc system with CCC control: (a) chopper rectifiers; (b) thyristor rectifiers.

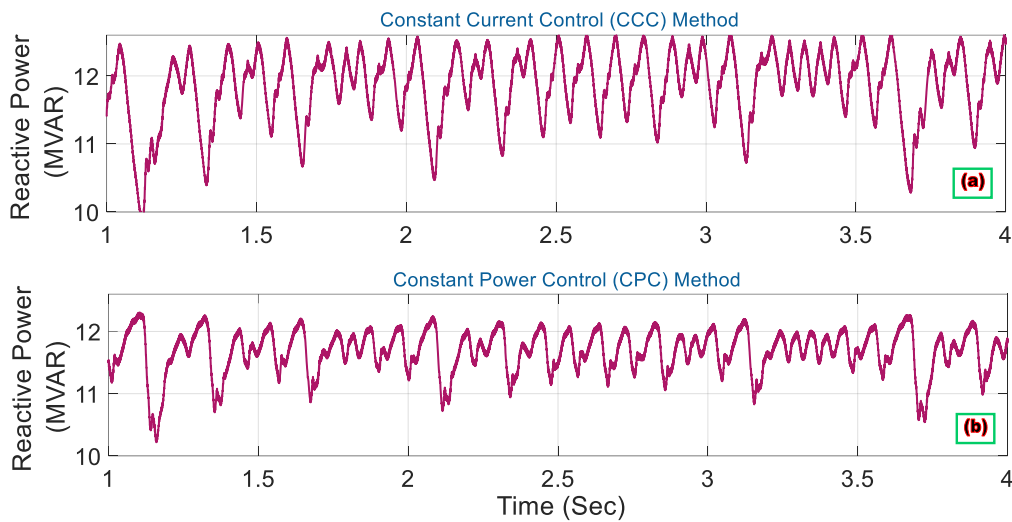


Figure 20. Reactive power of DC arc system based on chopper rectifiers with: (a) CCC; (b) CPC.

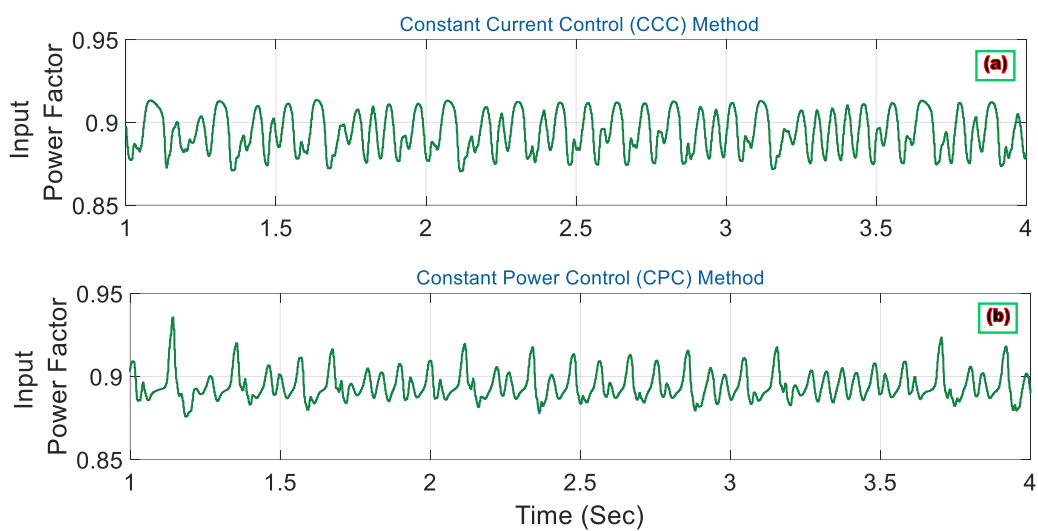


Figure 21. Input power factor of DC arc system based on chopper rectifiers with: (a) CCC; (b) CPC.

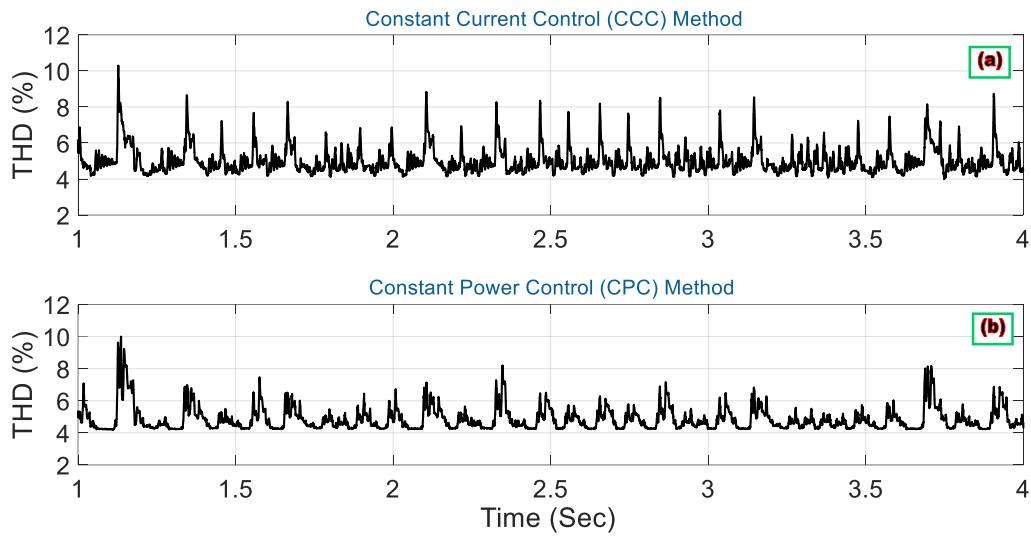


Figure 22. Input current THD of DC arc system based on chopper rectifiers with: (a) CCC; (b) CPC.

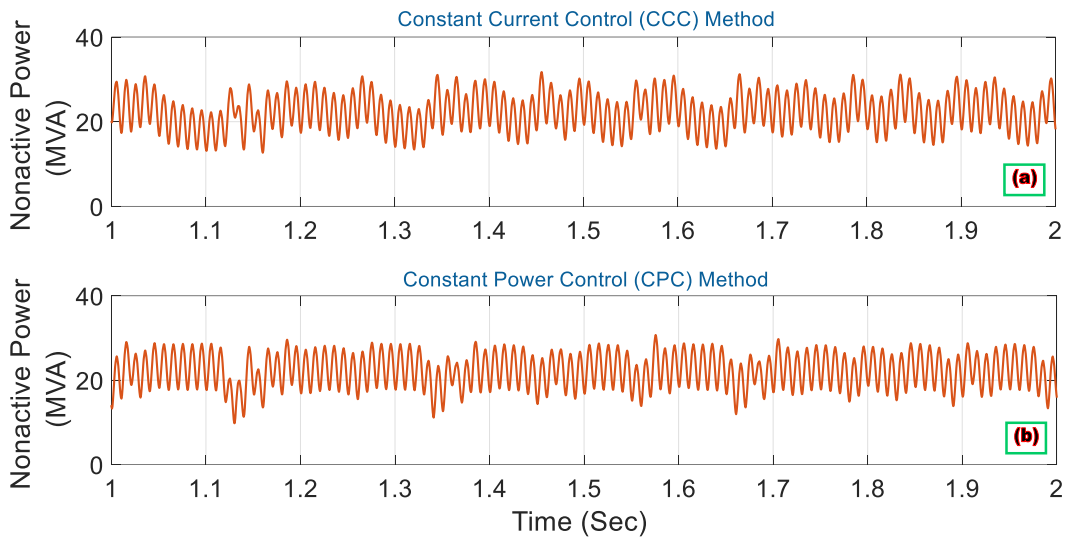


Figure 23. Non-active power of DC arc system based on chopper rectifiers with: (a) CCC; (b) CPC.

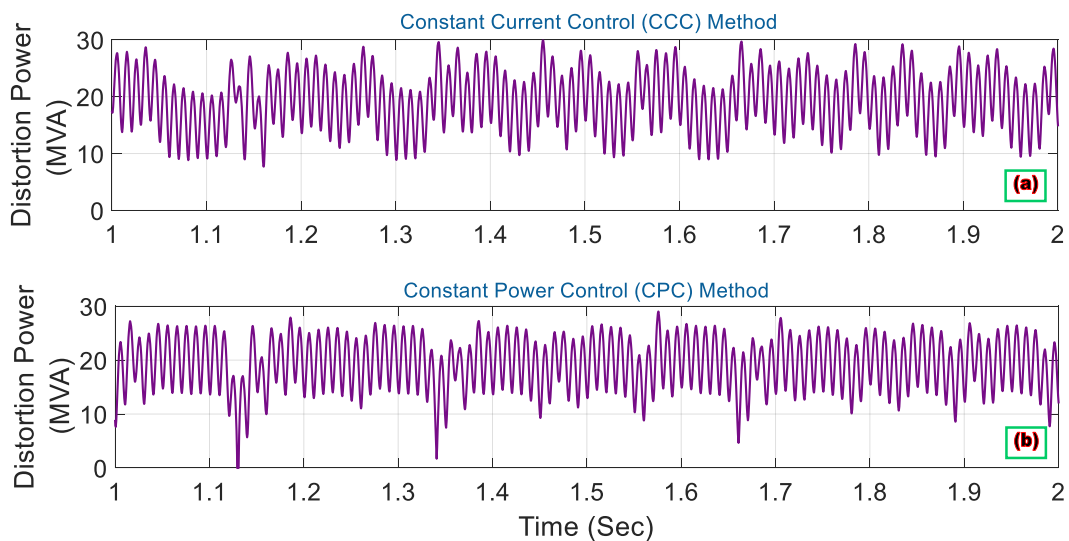


Figure 24. Distortion power of DC arc system based on chopper rectifiers with: (a) CCC; (b) CPC.

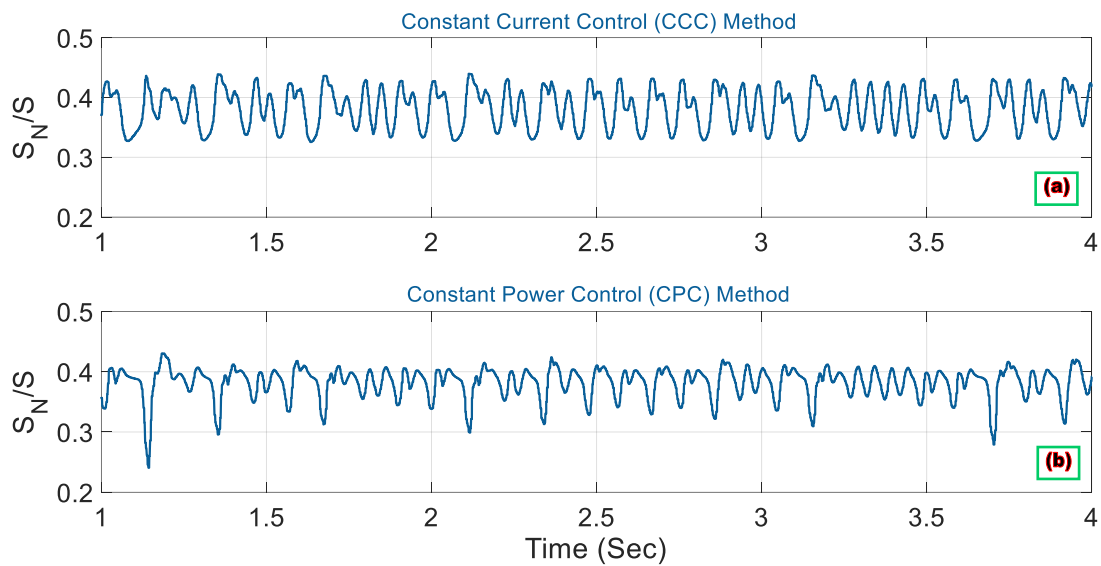


Figure 25.  $S_N/S$  index in DC arc system based on chopper rectifiers with: (a) CCC; (b) CPC.

5.3. Discussion

In Figure 26, a comparison of non-active power and distortion power in the DC arc furnace system for chopper rectifiers and thyristor rectifiers is presented with CCC and CPC control methods. As shown in Figure 26, the maximum non-active power was reduced from 49.5 MVA in thyristor rectifiers to 30.7 MVA in chopper rectifiers with the CPC method. For the CCC method, the maximum non-active power was reduced from 44.1 MVA in thyristor rectifier to 31.8 MVA in chopper rectifiers. Furthermore, the maximum distortion power was reduced from 37.1 MVA in thyristor rectifiers to 29 MVA in chopper rectifiers with the CPC method. The results are similar to the CCC method.

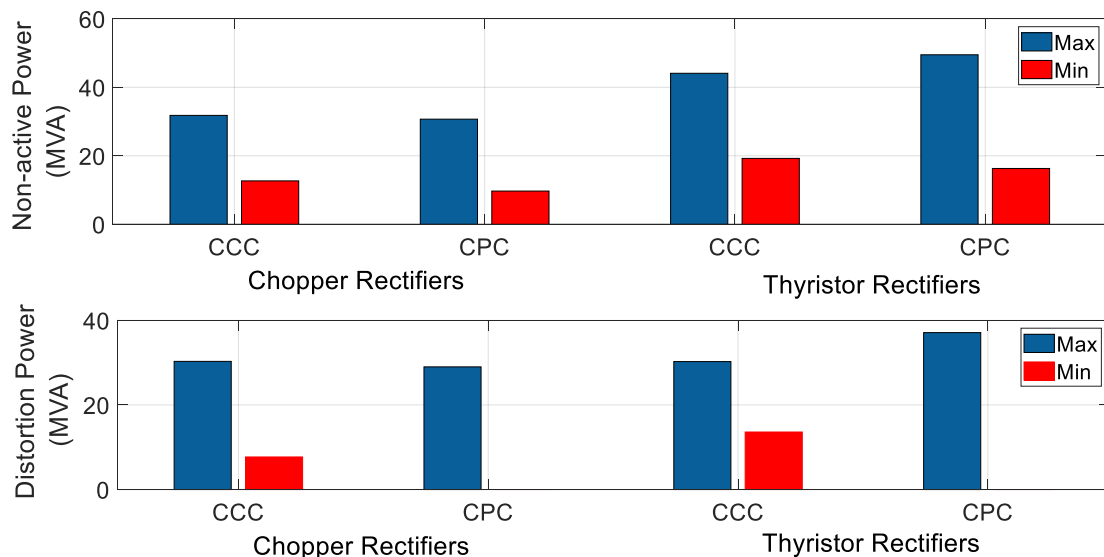


Figure 26. Comparison of non-active power and distortion power of DC arc furnace system for chopper rectifiers and thyristor rectifiers with CCC and CPC control.

In Table 1 and Figure 27, a comparison of input current THD and input voltage THD of the AC side in the DC arc furnace system for chopper rectifiers and thyristor rectifiers is provided with CCC and CPC control methods. As shown in Figure 27, the average current THD is reduced from 16.55% in the thyristor rectifiers to 8.40% in the chopper rectifiers with the CCC method and from 19.27% in the thyristor rectifiers to 7.38% in the chopper

rectifiers with the CPC method. Moreover, the average voltage THD is reduced from 5.67% in the thyristor rectifier to 3.02% in the chopper rectifiers with the CCC method. The result is similar to the CPC method.

**Table 1.** Comparison of input current THD and input voltage THD of AC side in DC arc furnace system for chopper rectifiers and thyristor rectifiers with CCC and CPC control.

Feeding System	Control Method	Current THD (%)			Voltage THD (%)		
		Minimum	Maximum	Average	Minimum	Maximum	Average
Chopper rectifiers	CCC	6.26	31.15	8.40	1.88	29.90	3.02
	CPC	5.19	33.74	7.38	1.89	29.91	3.02
Thyristor rectifiers	CCC	13.26	44.44	16.55	4.57	29.90	5.67
	CPC	14.79	48.02	19.27	4.60	29.93	5.70

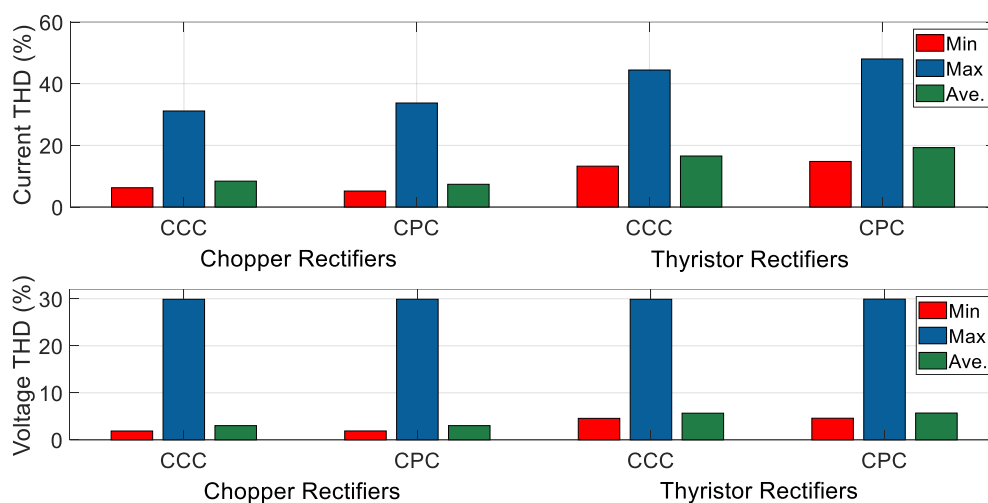


**Figure 27.** Comparison of input current THD and input voltage THD of AC side in DC arc furnace system for chopper rectifiers and thyristor rectifiers with CCC and CPC control.

According to the results, the power and THD values are lower in power supply systems with chopper rectifiers than in thyristor rectifiers.

## 6. Conclusions

In this paper, the common feeding systems of DC electric arc furnaces, including the feeding system based on thyristor rectifiers and the feeding system based on diode rectifiers with DC choppers, were studied, and then the effects of each of these feeding systems on various power quality indexes were investigated. Simulation results manifest that the DC chopper rectifier feeding system for DC arc furnaces, with constant current or constant power control methods, will have lower deviation compared to the specified reference value. Moreover, the results show that the reactive power absorbed from the network is significantly reduced in the case of the chopper feeding system. Therefore, the input power factor is also considerably improved in this case. In addition, it has been shown that the THD related to the input currents is substantially reduced by using a feeding system based on chopper units. According to the results, the average current THD is reduced from 16.55% in the thyristor rectifiers to 8.40% in the chopper rectifiers with the CCC method and from 19.27% in the thyristor rectifiers to 7.38% in the chopper rectifiers with the CPC method. Moreover, the average voltage THD is reduced from 5.67% in the thyristor rectifiers to 3.02% in the chopper rectifiers with the CCC method. The result is similar to the CPC method. Moreover, in the conditions of using the DC arc feeding system based on chopper rectifiers, in the CPC method, the reactive power fluctuations and the power factor are less than in the CCC method. Finally, it has been shown that in the case of the power supply

system based on chopper rectifiers, the non-active ( $N$ ) and distortion ( $D$ ) powers have smaller values than the power supply system based on thyristor rectifiers. The maximum non-active power is 37.9% lower in chopper rectifiers than in thyristor rectifiers for the CPC method. For the CCC method, the maximum non-active power is 27.9% lower in chopper rectifiers than in thyristor rectifiers. The maximum distortion power is 21.8% lower in chopper rectifiers than in thyristor rectifiers for the CPC method. The results are similar to the CCC method.

All in all, it can be concluded that from the point of view of network issues that power supply systems based on diode rectifiers and DC choppers are superior to types based on thyristor rectifiers.

**Author Contributions:** Conceptualization, P.H. and C.G.; methodology, P.H.; software, P.H.; validation, P.H. and C.G.; formal analysis, P.H. and C.G.; investigation, P.H.; data curation, C.G.; writing—original draft preparation, P.H.; writing—review and editing, P.H., C.G. and J.R.; supervision, J.R.; project administration, J.R. All authors have read and agreed to the published version of the manuscript.

**Funding:** This research received no external funding.

**Acknowledgments:** C. Garcia and J. Rodriguez acknowledge the support of ANID through projects FB0008 Advanced Center for Electrical and Electronics Engineering, Regular Fondecyt 1210208, and 1221293.

**Conflicts of Interest:** The authors declare no conflict of interest.

## Appendix A

Figure A1 shows a detailed structure of the power supply system based on diode rectifiers and buck choppers.

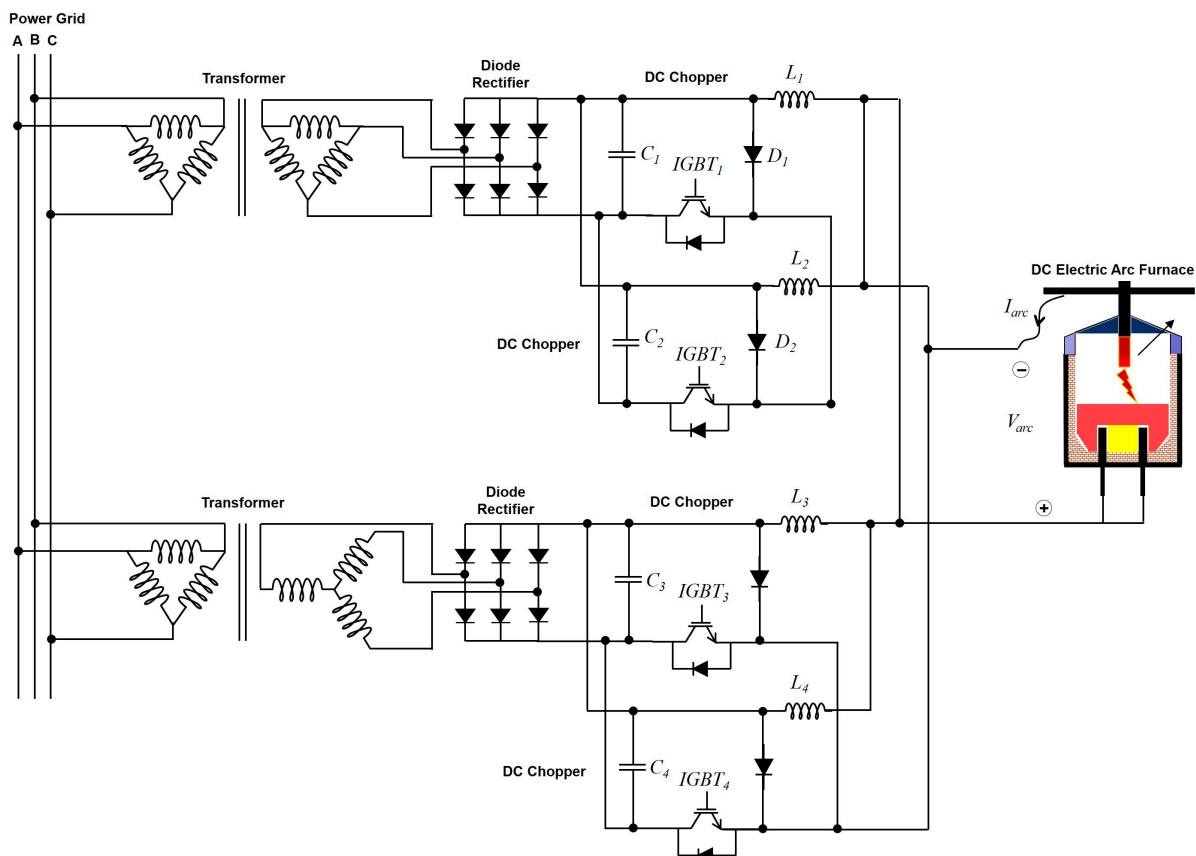


**Figure A1.** Block diagram of the power supply system based on diode rectifiers and DC choppers.

## Appendix B

Considering that the DC current usually has very high values and the current fluctuations are controlled by the power converter, the DC arc voltage ( $v_a$ ) can be written as [22]:

$$v_a \cong v_a^{\text{dc}} + \Delta v_a \quad (\text{A1})$$

in which  $v_a^{\text{dc}}$  is the constant part of the arc voltage, and  $\Delta v_a$  is the time-varying part related to the changes in the arc length  $l_0$ .

According to the Lorenz chaotic model, a set of three state equations can be introduced as follows [22]:

$$\begin{aligned} \dot{x} &= -\sigma x + \sigma y \\ \dot{y} &= -xz + rx - y \\ \dot{z} &= xy - bz \end{aligned} \quad (\text{A2})$$

where  $x$ ,  $y$ , and  $z$  are the state variables.  $\sigma$ ,  $b$ , and  $r$  are the Lorenz model parameters and should be properly specified for correct simulation of the DC arc. Variable  $z$  is supposed as an output, and  $\Delta v_a$  is determined by shifting and scaling the variable  $z$ . Finally, the DC arc voltage of the chaotic model is determined by adding the measured  $v_a^{\text{dc}}$  value to the produced signal  $\Delta v_a$  [22]. Simulation parameters are taken from [2].

## References

1. Ververne, I.; Van Reusel, K.; Belmans, R. Electric arc furnace modeling from a “power quality” point of view. In Proceedings of the 9th International Conference on Electrical Power Quality and Utilization, Barcelona, Spain, 9–11 October 2007. [\[CrossRef\]](#)
2. Dehestani, A.; Shoulaie, A. A Novel Feeding Topology for DC Electric Arc Furnaces Utilizing PWM-AC Choppers. *Int. Trans. Electr. Energ. Syst.* **2014**, *24*, 520–546. [\[CrossRef\]](#)
3. Dehestani, A.; Abdollahi Arjanaki, A.; Alizadeh, M.R. A New Matrix Converter-Based Feeding System for DC Electric Arc Furnaces and a Comprehensive Comparison between Different Types of Feeding Topologies. *Int. Trans. Electr. Energ. Syst.* **2019**, *30*, e12280. [\[CrossRef\]](#)
4. Ladoux, P.; Postiglione, G.; Foch, H.; Nuns, J. A Comparative Study of AC/DC Converters for High-Power DC Arc Furnace. *IEEE Trans. Ind. Electron.* **2005**, *52*, 747–757. [\[CrossRef\]](#)
5. Carpinelli, G.; Russo, A. Comparison of Some Active Devices for the Compensation of DC Arc Furnaces. In Proceedings of the Power Tech Conference Proceedings, Bologna, Italy, 23–26 June 2003. [\[CrossRef\]](#)
6. Olczykowski, Z.; Lukasik, Z. Evaluation of Flicker of Light Generated by Arc Furnaces. *Energies* **2021**, *14*, 3901. [\[CrossRef\]](#)
7. Lukasik, Z.; Olczykowski, Z. Estimating the Impact of Arc Furnaces on the Quality of Power in Supply Systems. *Energies* **2020**, *13*, 1462. [\[CrossRef\]](#)
8. Olczykowski, Z. Electric Arc Furnaces as a Cause of Current and Voltage Asymmetry. *Energies* **2021**, *14*, 5058. [\[CrossRef\]](#)
9. Olczykowski, Z. Arc Voltage Distortion as a Source of Higher Harmonics Generated by Electric Arc Furnaces. *Energies* **2022**, *15*, 3628. [\[CrossRef\]](#)
10. Jebaraj, B.S.; Bennet, J.; Kannadasan, R.; Alsharif, M.H.; Kim, M.-K.; Aly, A.A.; Ahmed, M.H. Power Quality Enhancement in Electric Arc Furnace Using Matrix Converter and Static VAR Compensator. *Electronics* **2021**, *10*, 1125. [\[CrossRef\]](#)
11. Pajic, S.; Emanuel, A.E. Effect of Neutral Path Power Losses on the Apparent Power Definitions: A Preliminary Study. *IEEE Trans. Power Deliv.* **2009**, *24*, 517–523. [\[CrossRef\]](#)
12. Naseri, F.; Samet, H. A comparison study of high power IGBT-based and thyristor-based AC to DC converters in medium power DC arc furnace plants. In Proceedings of the 9th International Conference on Compatibility and Power Electronics (CPE), Costa da Caparica, Portugal, 24–26 June 2015; pp. 14–19. [\[CrossRef\]](#)
13. Dehestani, A.; Mohamadian, S.; Shoulaie, A. Unbalance Assessment and Apparent Power Decomposition in The Electric System of Interharmonic-Producing Loads. *Int. Trans. Electr. Energ. Syst.* **2014**, *24*, 246–263. [\[CrossRef\]](#)
14. Dehestani, A.; Shoulaie, A. Power Quality Improvement in DC Electric Arc Furnace Plants Utilizing Multi-Phase Transformers. *Int. Trans. Electr. Energ. Syst.* **2013**, *23*, 1233–1253. [\[CrossRef\]](#)
15. Abdulveleev, I.R.; Khramshin, T.R.; Kornilov, G.P.; Abdulveleeva, R.R. Experimental Study of the Impact of a DC Electric Arc Furnace on a Power Grid. In Proceedings of the International Conference on Industrial Engineering, Applications and Manufacturing (ICIEAM), Sochi, Russia, 17–21 May 2021; pp. 214–218. [\[CrossRef\]](#)
16. Bracale, A.; Caramia, P.; De Falco, P.; Carpinelli, G.; Russo, A. DC Electric Arc Furnace Modeling for Power Quality Indices Assessment. In Proceedings of the 19th International Conference on Harmonics and Quality of Power (ICHQP), Dubai, United Arab Emirates, 6–7 July 2020. [\[CrossRef\]](#)
17. Bracale, A.; Caramia, P.; Carpinelli, G.; De Falco, P.; Russo, A. Comparison of DC Electric Arc Furnace Chaotic Models for Power Quality Indices Assessment. *IEEE Trans. Ind. Appl.* **2021**, *57*, 6713–6721. [\[CrossRef\]](#)

18. Abdulveleev, I.R.; Kornilov, G.P.; Khramshin, T.R. Research of DC Electric Arc Furnace with Commutated Power Circuit. In Proceedings of the International Conference on Industrial Engineering, Applications and Manufacturing (ICIEAM), Sochi, Russia, 18–22 May 2020; pp. 1–7. [[CrossRef](#)]
19. Lazaroiu, G.C.; Zaninelli, D. A Control System for DC Arc Furnaces for Power Quality Improvements. *Electr. Power Syst. Res.* **2010**, *80*, 1498–1505. [[CrossRef](#)]
20. Rodriguez, J.R.; Pontt, J.; Silva, C.; Wiechmann, E.P.; Hammond, P.W.; Santucci, F.W.; Alvarez, R.; Musalem, R.; Kouro, S.; Lezana, P. Large Current Rectifiers: State of the Art and Future Trends. *IEEE Trans. Ind. Electron.* **2005**, *52*, 738–746. [[CrossRef](#)]
21. Fu, T.H.; Wu, C.J. Load characteristics analysis of AC and DC arc furnaces using various power definitions and statistic method. *IEEE Trans. Power Deliv.* **2002**, *17*, 1099–1105. [[CrossRef](#)]
22. Carpinelli, G.; Iacovone, F.; Russo, A.; Varilone, P. Chaos-Based Modeling of DC Arc Furnaces for Power Quality Issues. *IEEE Trans. Power Deliv.* **2004**, *19*, 1869–1876. [[CrossRef](#)]

**Disclaimer/Publisher’s Note:** The statements, opinions and data contained in all publications are solely those of the individual author(s) and contributor(s) and not of MDPI and/or the editor(s). MDPI and/or the editor(s) disclaim responsibility for any injury to people or property resulting from any ideas, methods, instructions or products referred to in the content.